

Numerical Simulations of the Jet in the Crab Nebula

A. Mignone¹, A. Ferrari¹,
E. Striani², M. Tavani²

¹Dipartimento di Fisica, Università di Torino

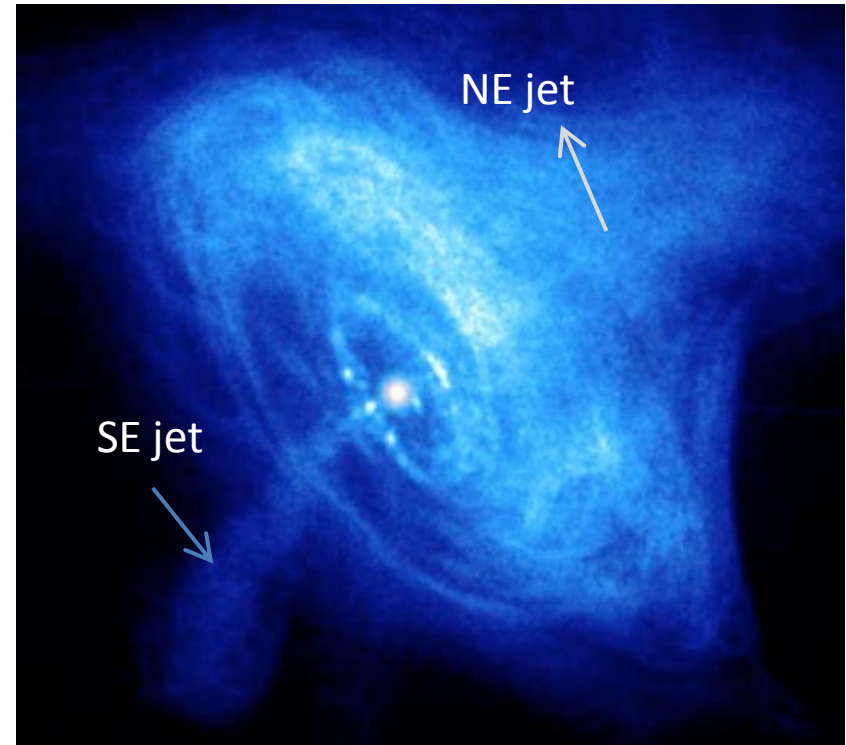
²IASF/IAPS università di tor vergata (roma)

Outline

1. *Observational Evidence*
 2. *Numerical Models of Relativistic MHD jets*
 3. *Results*
 4. *Summary*
-

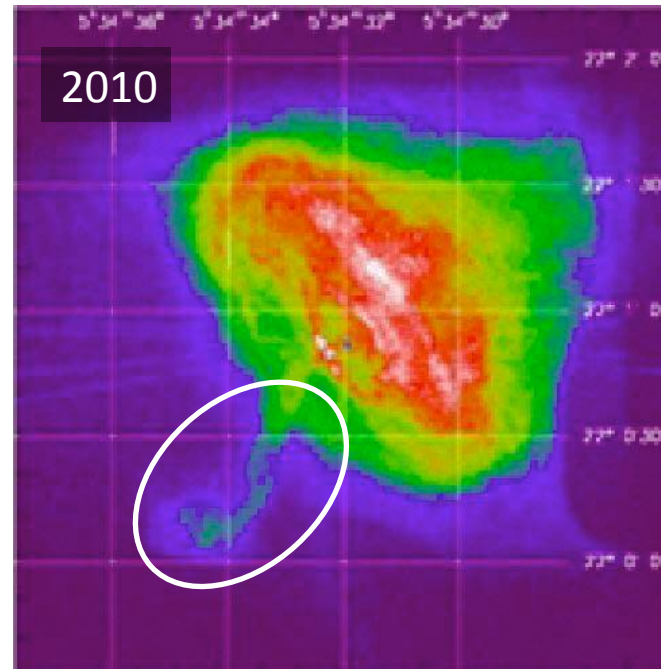
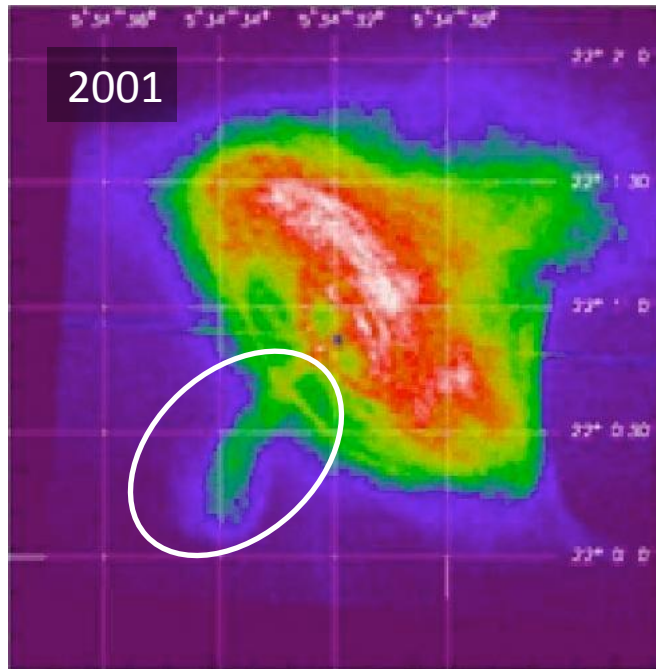
Observational Evidence

- X-ray observation (Chandra) show the emergence of a bipolar jets and extending to the SE and NEW of the pulsar;
- A region of diffuse emission (Anvil) may be associated with shocks and marks the base of the X-ray and optical jet;
- Knots of emission are seen along the jets;
- In the SE jet material flows with $v/c \sim 0.4$ slowing down to ~ 0.02 into the nebula;



Jet Wiggling

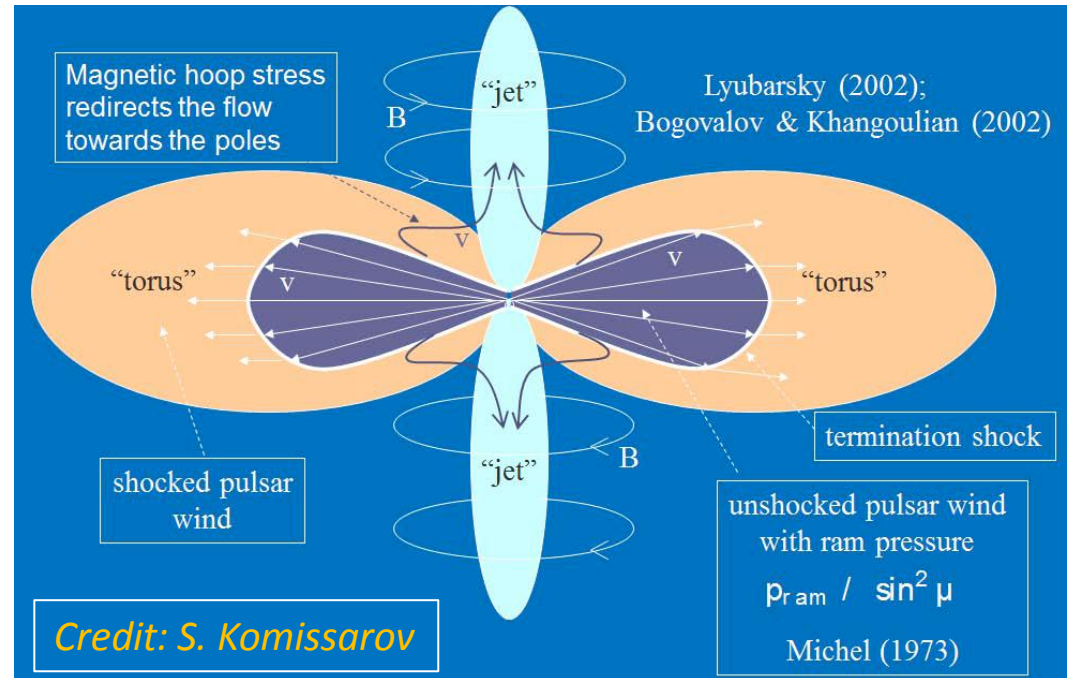
- SE jet morphology is “S” shaped and show remarkable time variability:



- → evidence for some kind of flow instability (Current Driven ?)

On the Origin of the Jet

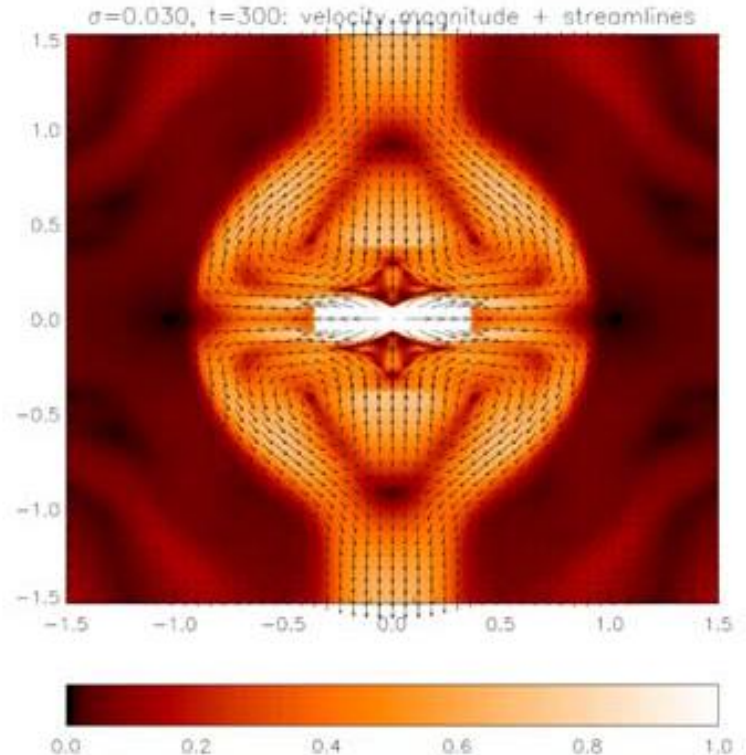
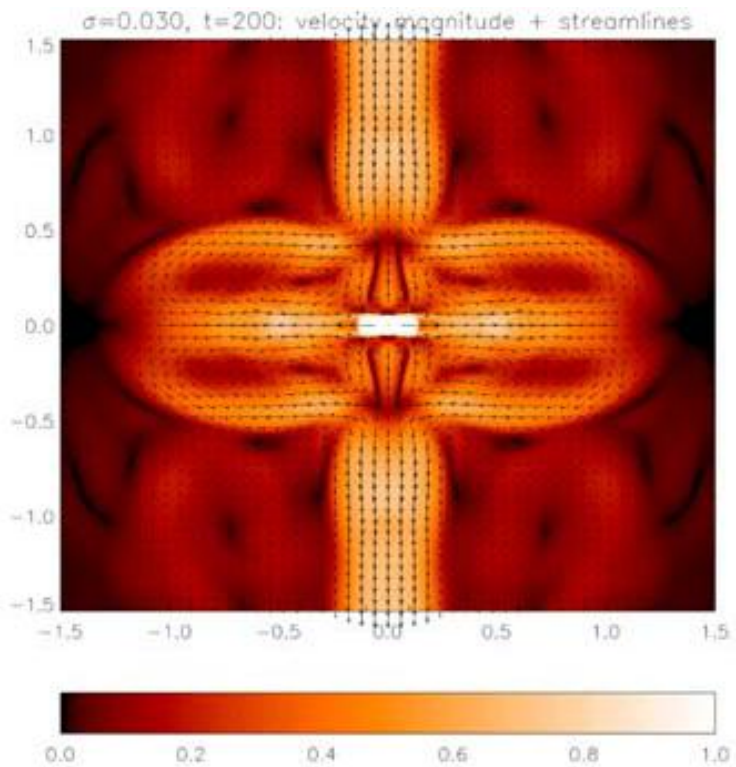
- Jet forms downstream of the wind termination shock;
- Magnetic fields confine matter towards polar axis;
→ **“tooth-paste”** effect: hoop stress of the azimuthal magnetic field carried by the wind (Lyubarsky 2002).



- Models confirmed by 2D axisymmetric numerical simulations (Komissarov & Lyubarski 2003,2004, Del Zanna et al. 2004, Bogovalov et al. 2005)

Jet Origin: previous results

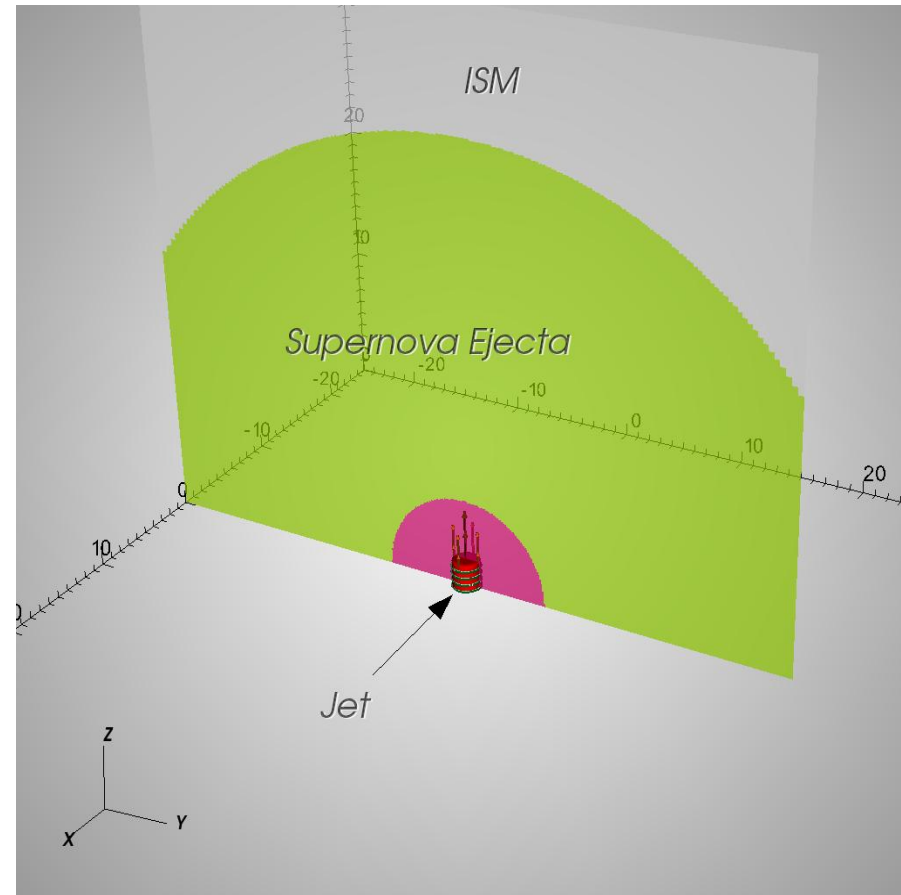
- For moderate/large $\sigma = B^2/(8\pi\rho c^2\gamma^2)$ magnetic hoop stress suppresses high velocity outflows in the equatorial plane and divert them towards the polar axis partially driving the super-fast jet¹



¹Del Zanna et al, A&A (2004) 421,1063

3D Jet models

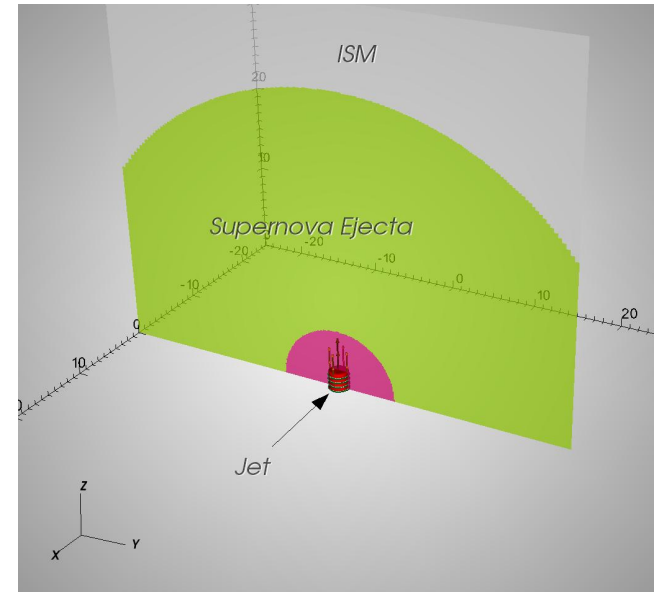
- Initial conditions from Del Zanna et al. (2004).
- Inside $0.2 < r < 1$ (ly): freely expanding supernova ejecta ($3 M_{\text{sun}}$, $E = 10^{51}$ erg)
- Jet enters at the lower z boundary;
- Pulsar wind structure not considered: jet already formed as the result of the collimation process;
- Jet radius $R_j = 3 \cdot 10^{16}$ cm
- Computational domain:
 $x, y \in [-25, 25] R_j / c$, $z \in [0, 80] R_j / c$;
($\approx 1.6 \times 2.5$ ly).



3D Jet models

➤ Jet flow modeled by 5 parameters:

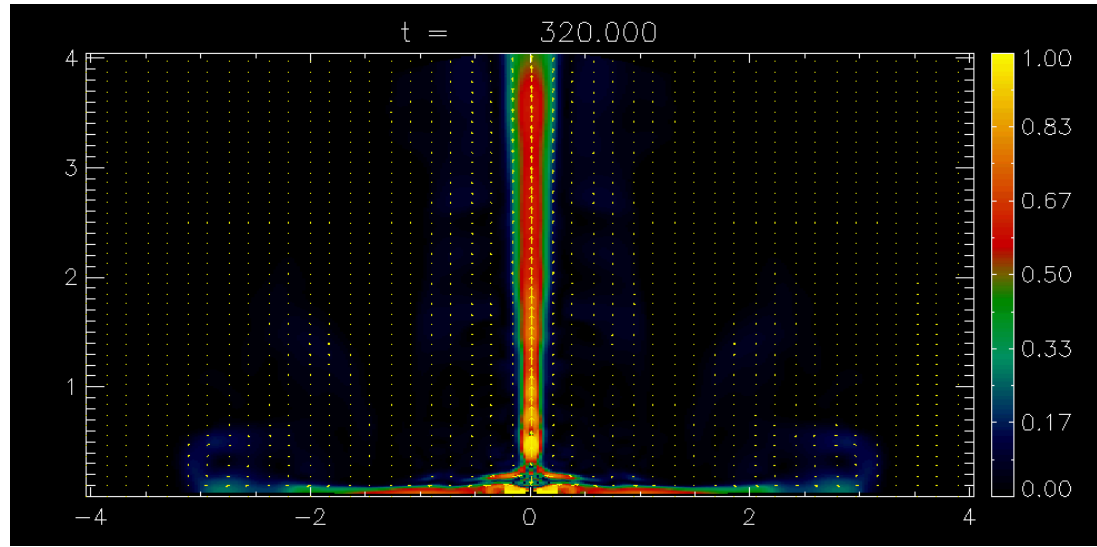
1. Sonic flow Mach number: $M_s = v_j / c_s$
2. Bulk Lorentz factor: $\gamma_j = (1 - v_j^2)^{-1/2}$
3. Jet/ambient dens. contrast: $\eta = \rho_j / \rho_e$
4. Magnetization: $\sigma = B^2 / (8\pi\rho\gamma^2)$
5. Pitch angle: $P = RB_z / B_\phi$



Parameter Constraints

➤ Parameters are constrained by 2D axisymmetric results

- $1.3 \lesssim M_s \lesssim 2 \rightarrow$ hot jet
- $2 \lesssim \gamma \lesssim 4$
- $\sigma = ?$
- Density contrast $\eta \lesssim 10^{-6}$
- Azimuthal field implies
Pitch $\rightarrow 0$ ($B_z = 0$)



➤ This leaves γ and σ as free parameters.

➤ We consider hollow ($\eta=10^{-6}$), hot ($M_s = 1.7$) jets initially carrying purely axial current ($B_\phi \neq 0, B_z = B_R = 0$).

➤ $\rho(R)$ and $B_\phi(R)$ set by radial momentum balance across the jet

Equations

- We solve the equations for a relativistic perfectly conducting fluid describing energy/momentum and particle conservation (relativistic MHD equations)

$$\frac{\partial}{\partial t}(\rho\gamma) + \nabla \cdot (\rho\gamma\mathbf{v}) = 0$$

$$\frac{\partial \mathbf{m}}{\partial t} + \nabla \cdot \left[w\gamma^2 \mathbf{v}\mathbf{v} - \mathbf{B}\mathbf{B} - \mathbf{E}\mathbf{E} \right] + \nabla p_t = 0$$

$$\frac{\partial \mathbf{B}}{\partial t} - \nabla \times (\mathbf{v} \times \mathbf{B}) = 0$$

$$\frac{\partial \mathcal{E}}{\partial t} + \nabla \cdot (\mathbf{m} - \rho\gamma\mathbf{v}) = 0$$

$$\mathcal{E} = w\gamma^2 - p + \frac{\mathbf{B}^2 + \mathbf{E}^2}{2} - \rho\gamma$$

- We use the PLUTO^{1,2} code for astrophysical fluid dynamics (freely distributed <http://plutocode.ph.unito.it>)
- Numerical resolution 320 x 320 x 768 zones (≈ 20 point on the jet)

Simulation Cases

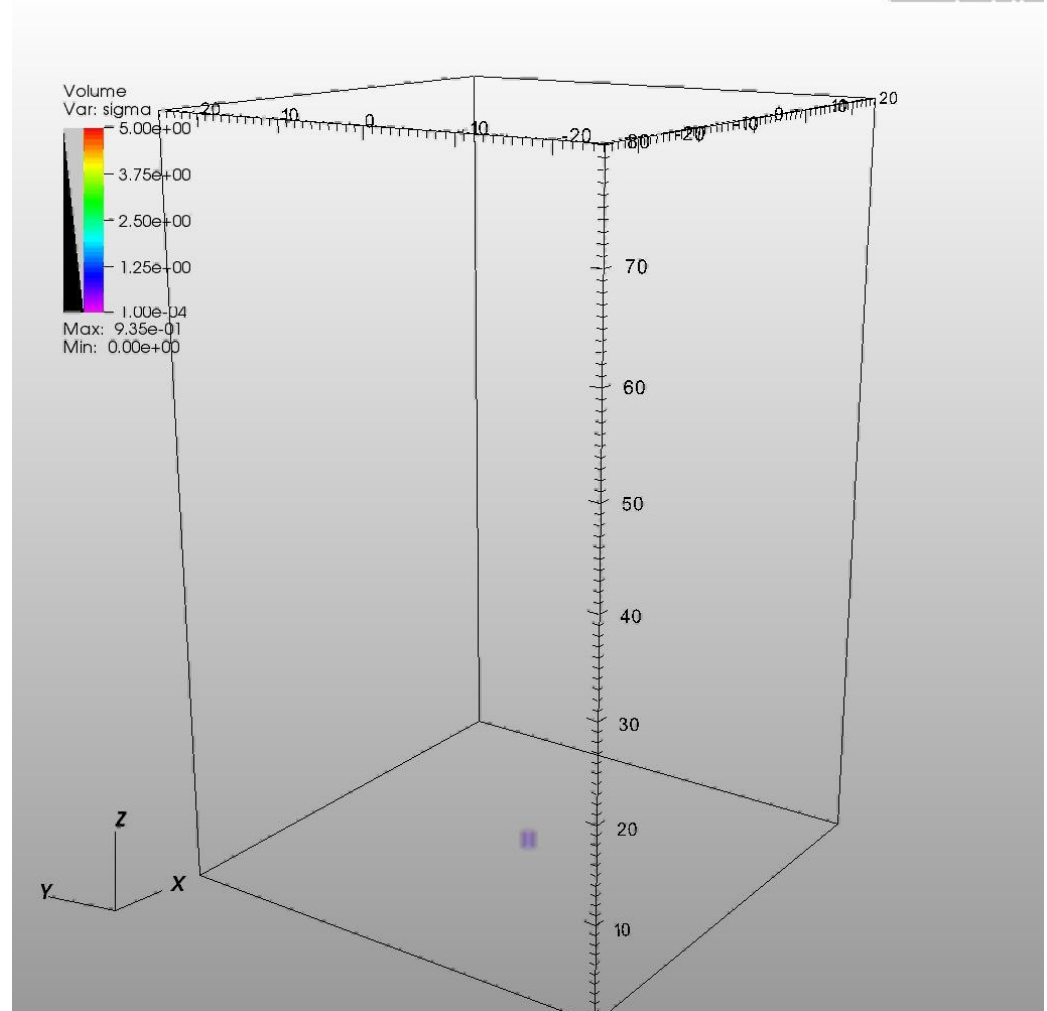
- We explore different values of Lorentz factor γ (= 2, 4) and magnetization σ (= 0.1, 1, 10) for a total of 6 different cases:

<i>Case</i>	γ	σ	<i>Plasma β</i>
A1	2	0.1	4.5
A2	2	1	0.6
A3	2	10	0.2
B1	4	0.1	11.4
B2	4	1	1.2
B3	4	10	0.15

Results: Case A2

Case	γ	σ
A1	2	0.1
A2	2	1
A3	2	10
B1	4	0.1
B2	4	1
B3	4	10

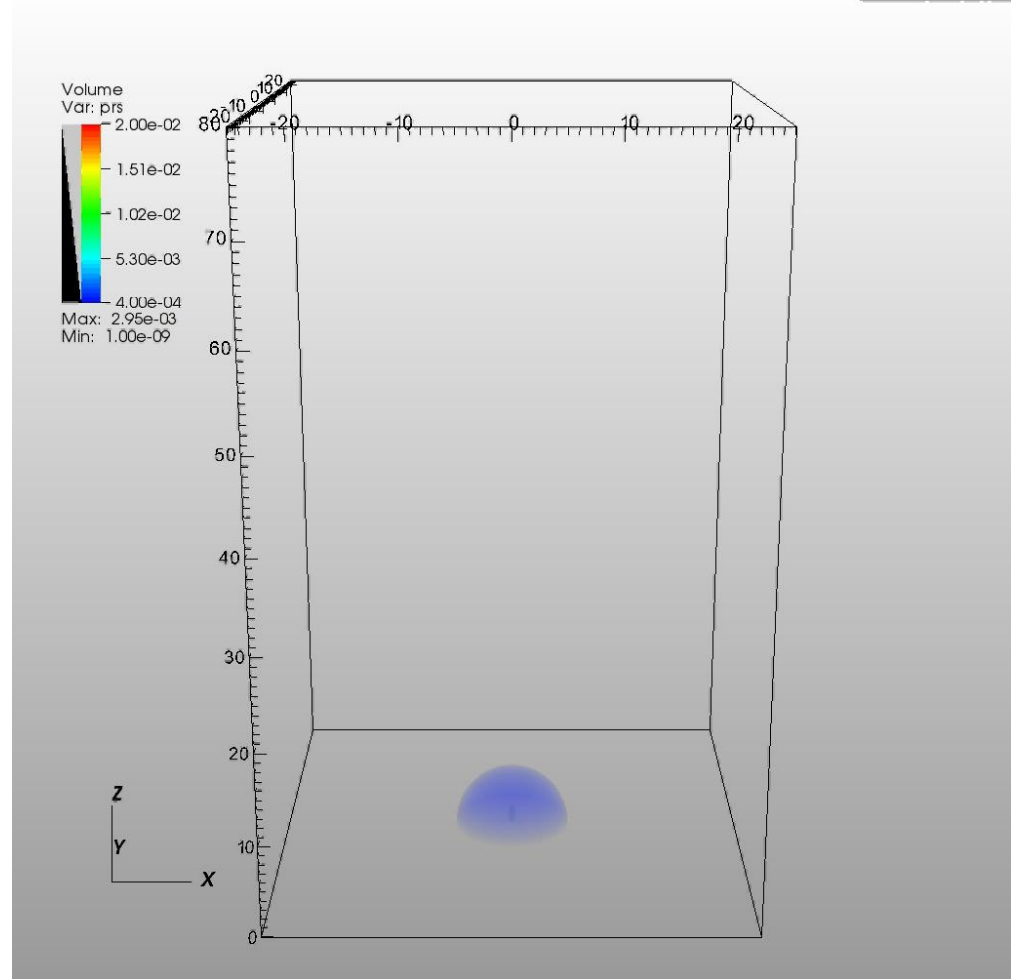
Sigma distribution



Results: Case A2

Case	γ	σ
A1	2	0.1
A2	2	1
A3	2	10
B1	4	0.1
B2	4	1
B3	4	10

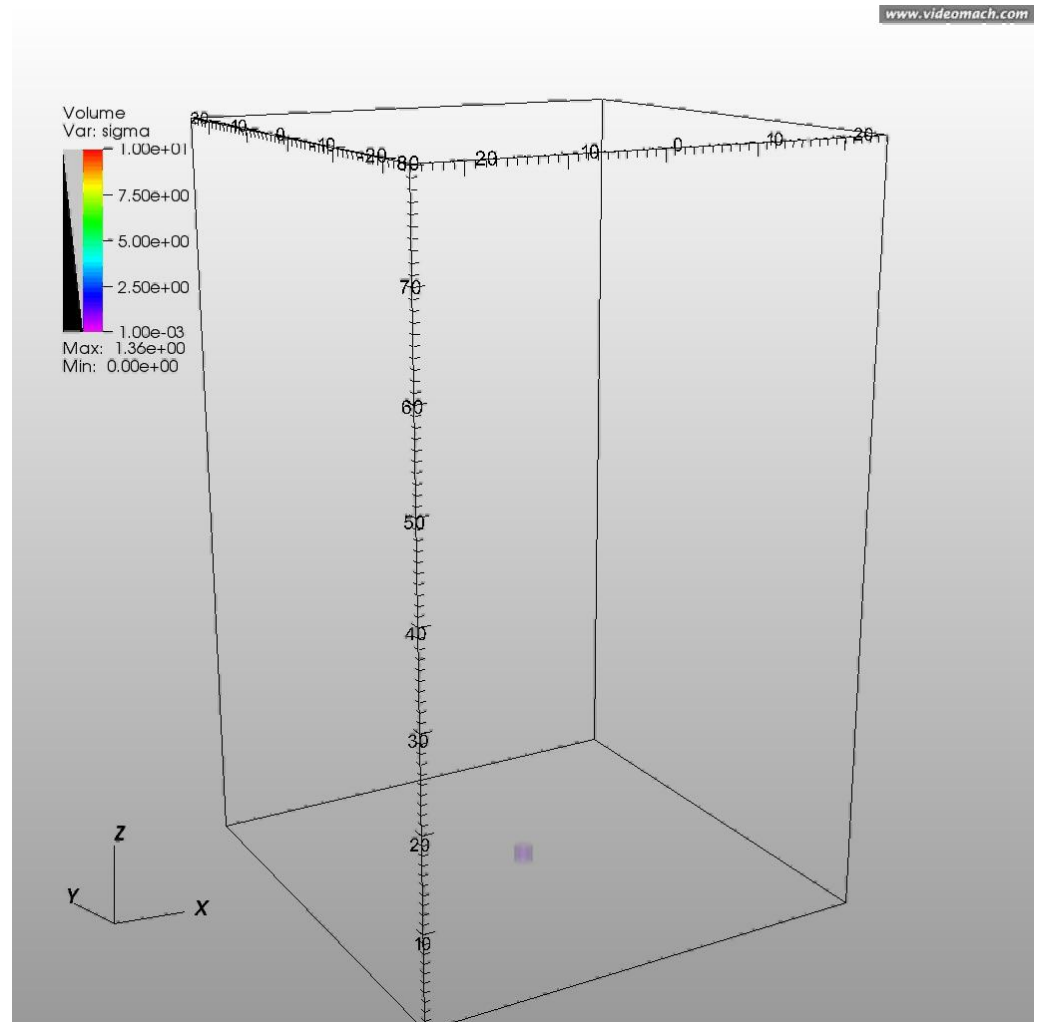
Pressure distribution



Results: Case B2

Case	γ	σ
A1	2	0.1
A2	2	1
A3	2	10
B1	4	0.1
B2	4	1
B3	4	10

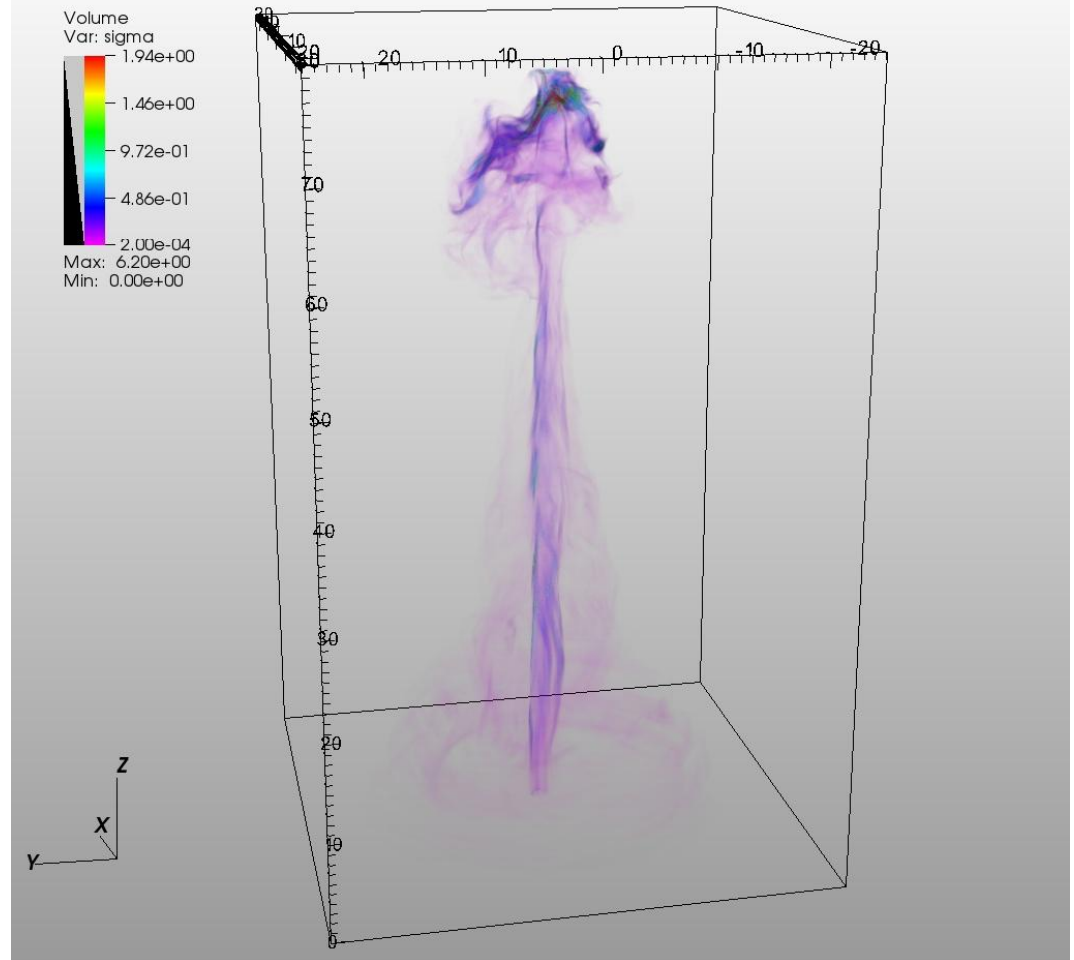
Sigma distribution



Results: Case B1

<i>Case</i>	γ	σ
A1	2	0.1
A2	2	1
A3	2	10
B1	4	0.1
B2	4	1
B3	4	10

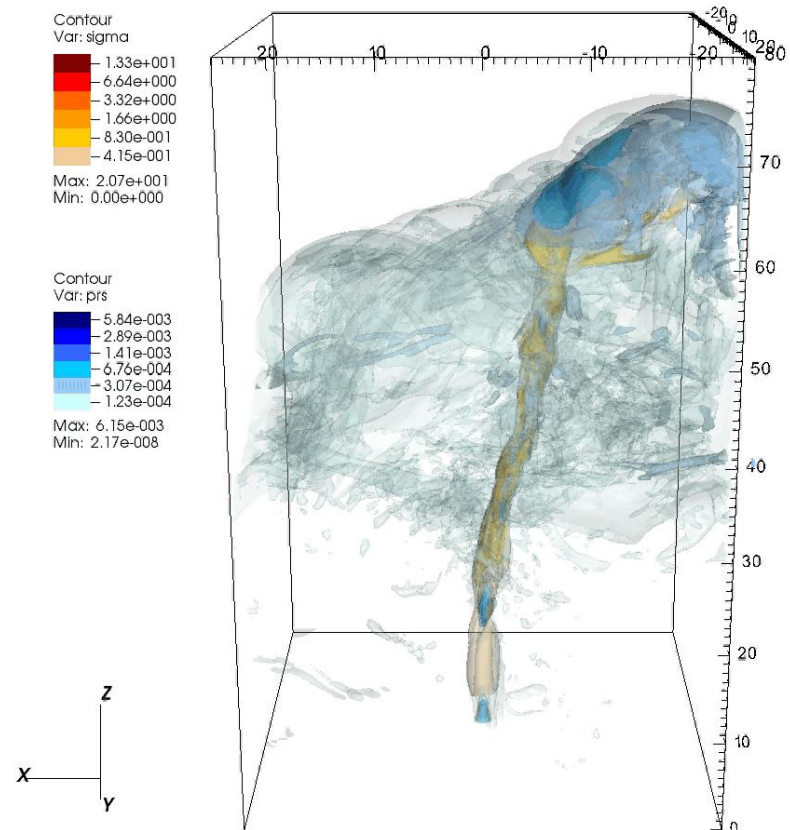
Sigma distribution



General Features

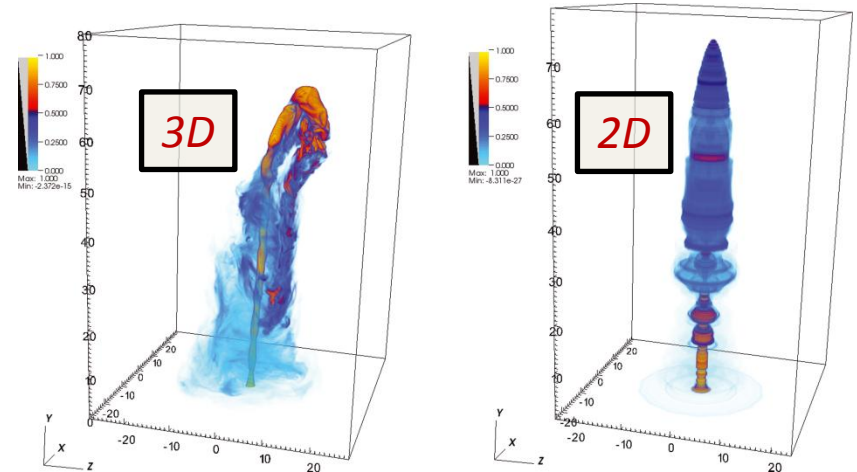
- Jets have small propagation speed ($0.02c - 0.08c$);
- Large over-pressurized turbulent cocoons;
- Collimated central spines moving at mildly relativistic speeds;
- Cocoon less magnetized than central spine;
- Large-scale deflections may be present.

www.videomach.com



General Features

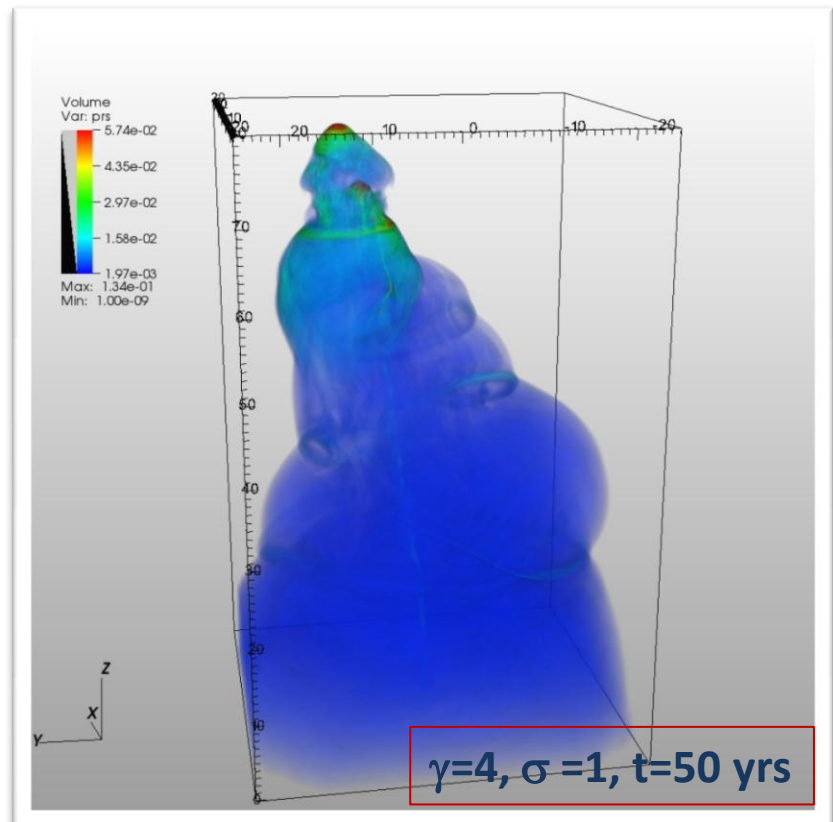
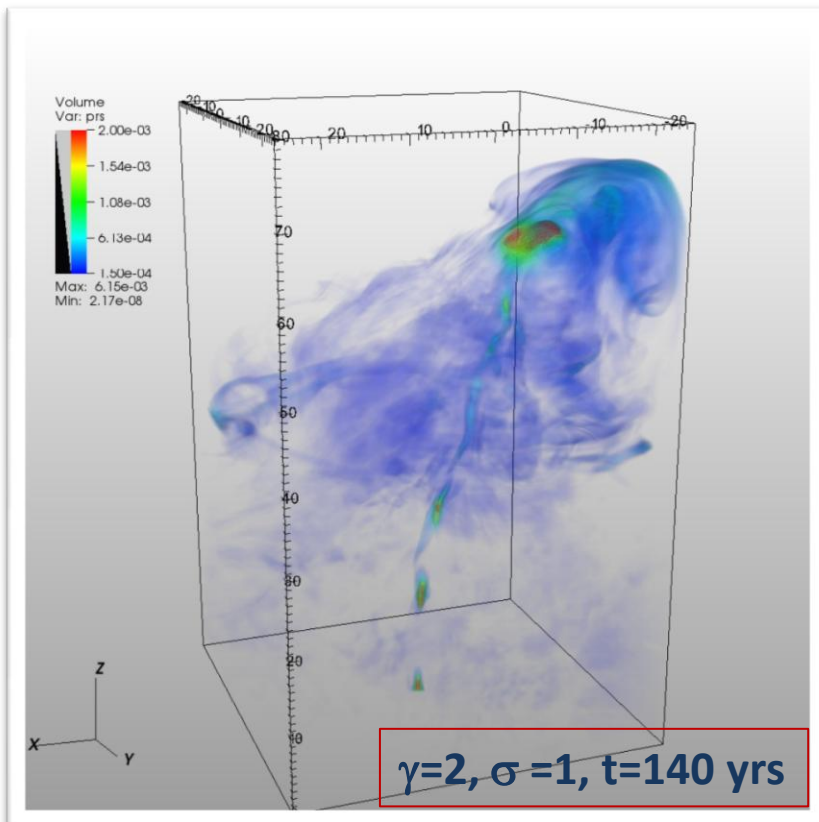
- 3D models very different from 2D counterparts¹:
- Strong toroidal configurations expected to become unstable to current driven modes. Most unstable mode $m=1$ (kink);
- Jet develops non-axisymmetric structures with large time-dependent deflections off the longitudinal axis;
- Deflection time-scale of the order of a few years;



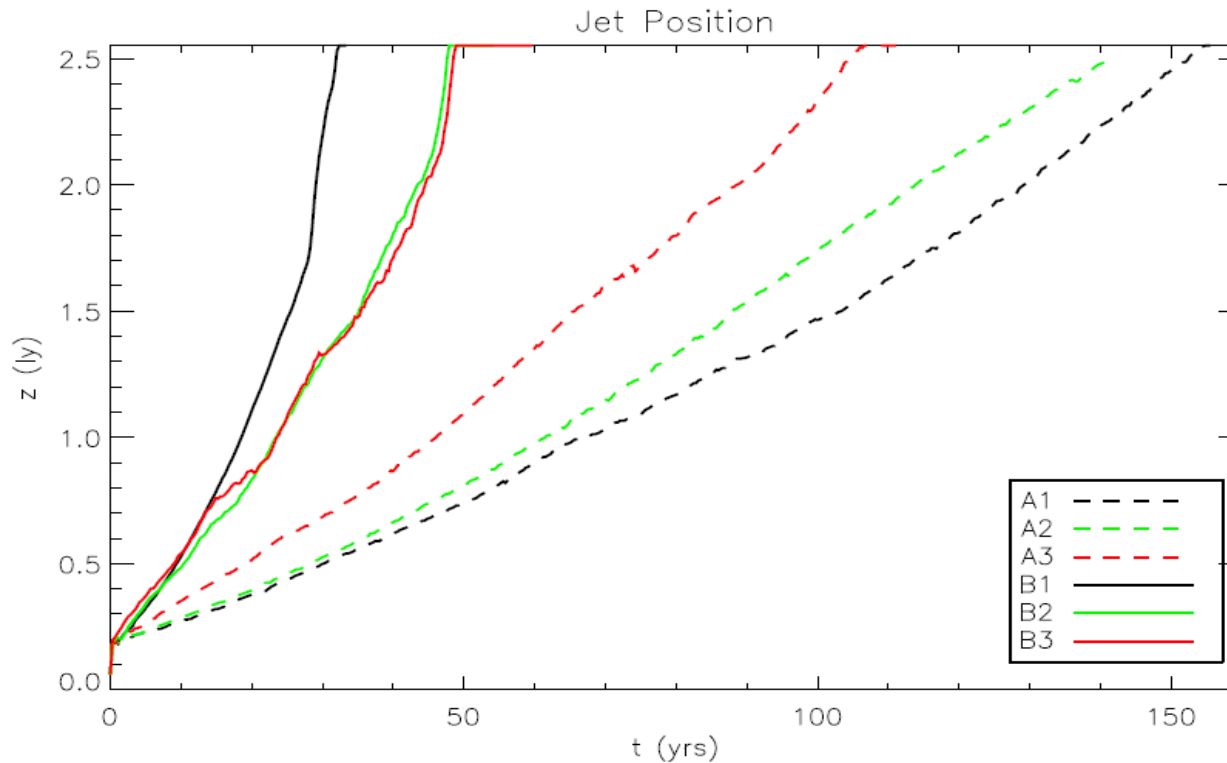
¹Mignone et al. MNRAS (2010), 402, 7

General Features

- Wiggling and deflection more pronounced at the terminal bow shock where magnetic field is amplified:



Jet Position



- Jets are slow because of large density contrast ($\rho_j / \rho_e < 10^{-6}$);
- Faster jets reach the outer edge of the expanding nebula.

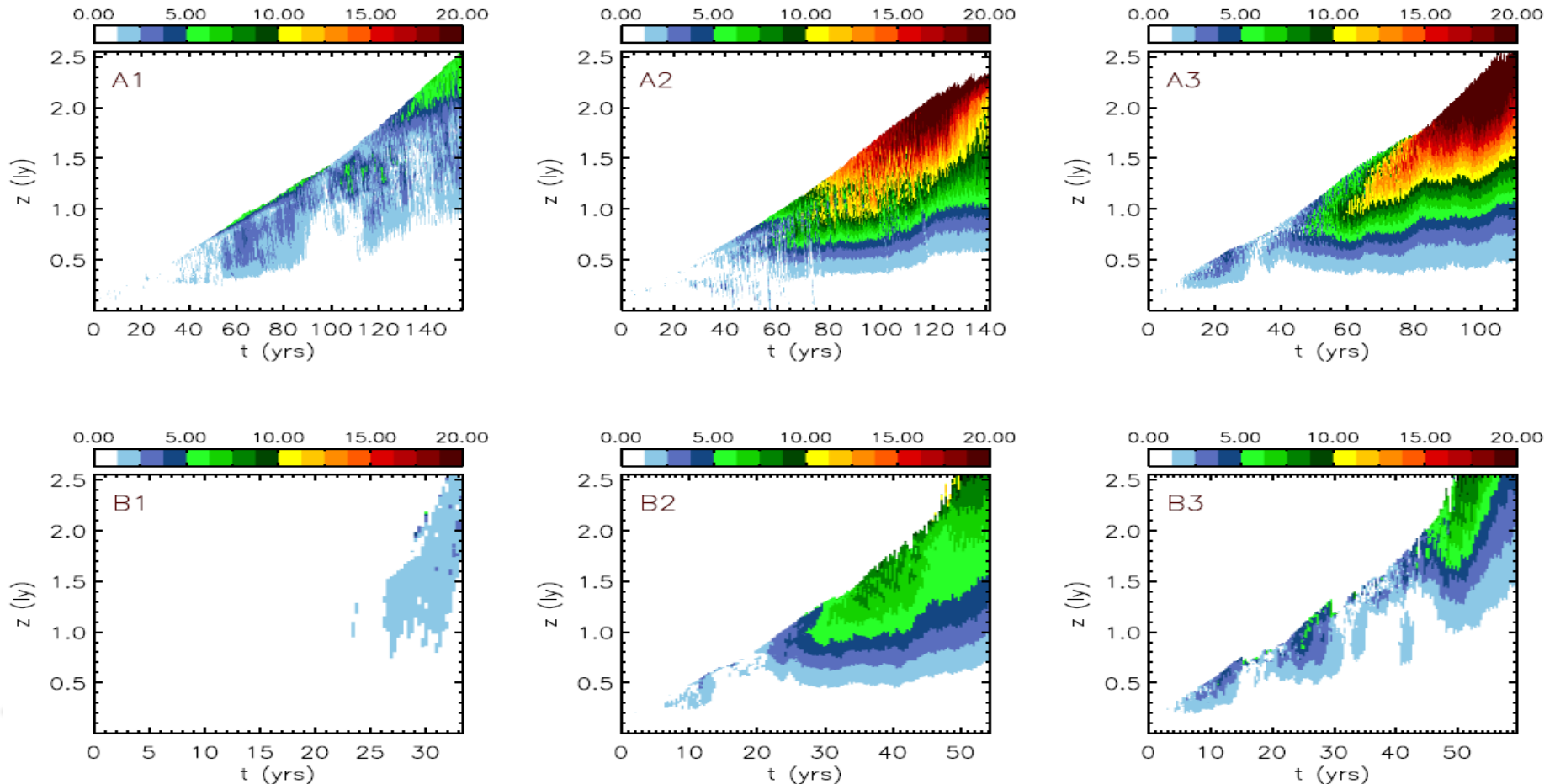
Jet Deflections

- Deflection is quantified using the baricenter:

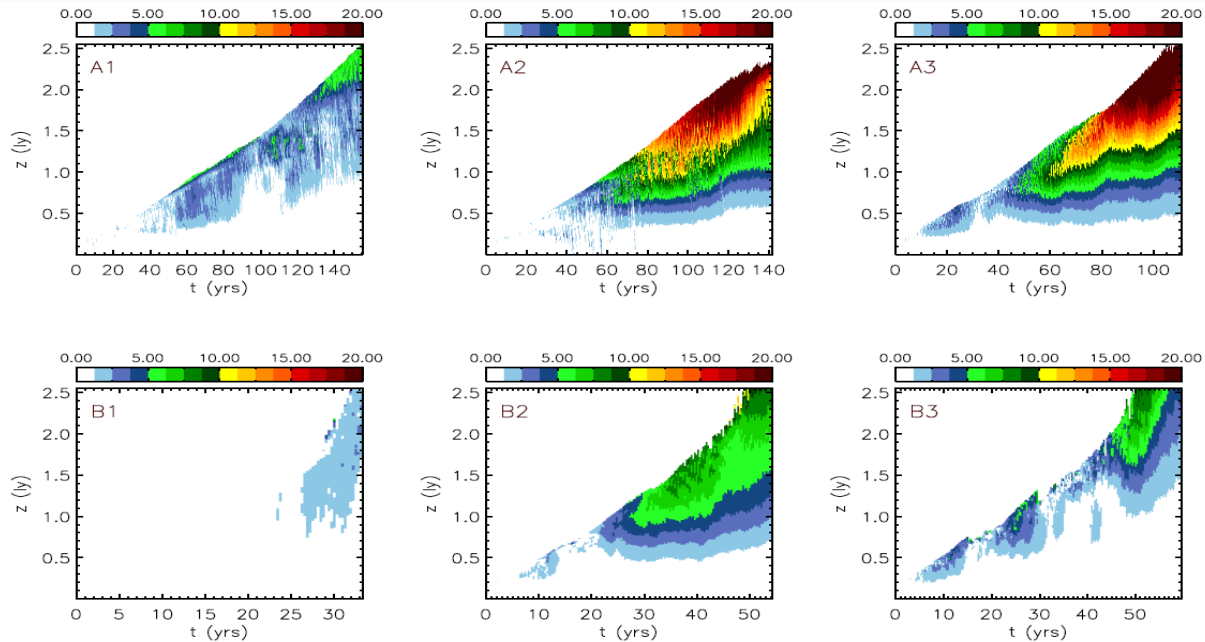
$$\bar{R}(z) \equiv \sqrt{\bar{x}^2(z) + \bar{y}^2(z)}$$

$$\bar{x}(z) = \frac{\int xQ(x, y, z)dx dy}{\int Q(x, y, z)dx dy}$$

$$\bar{y}(z) = \frac{\int yQ(x, y, z)dx dy}{\int Q(x, y, z)dx dy}$$



Jet Deflections

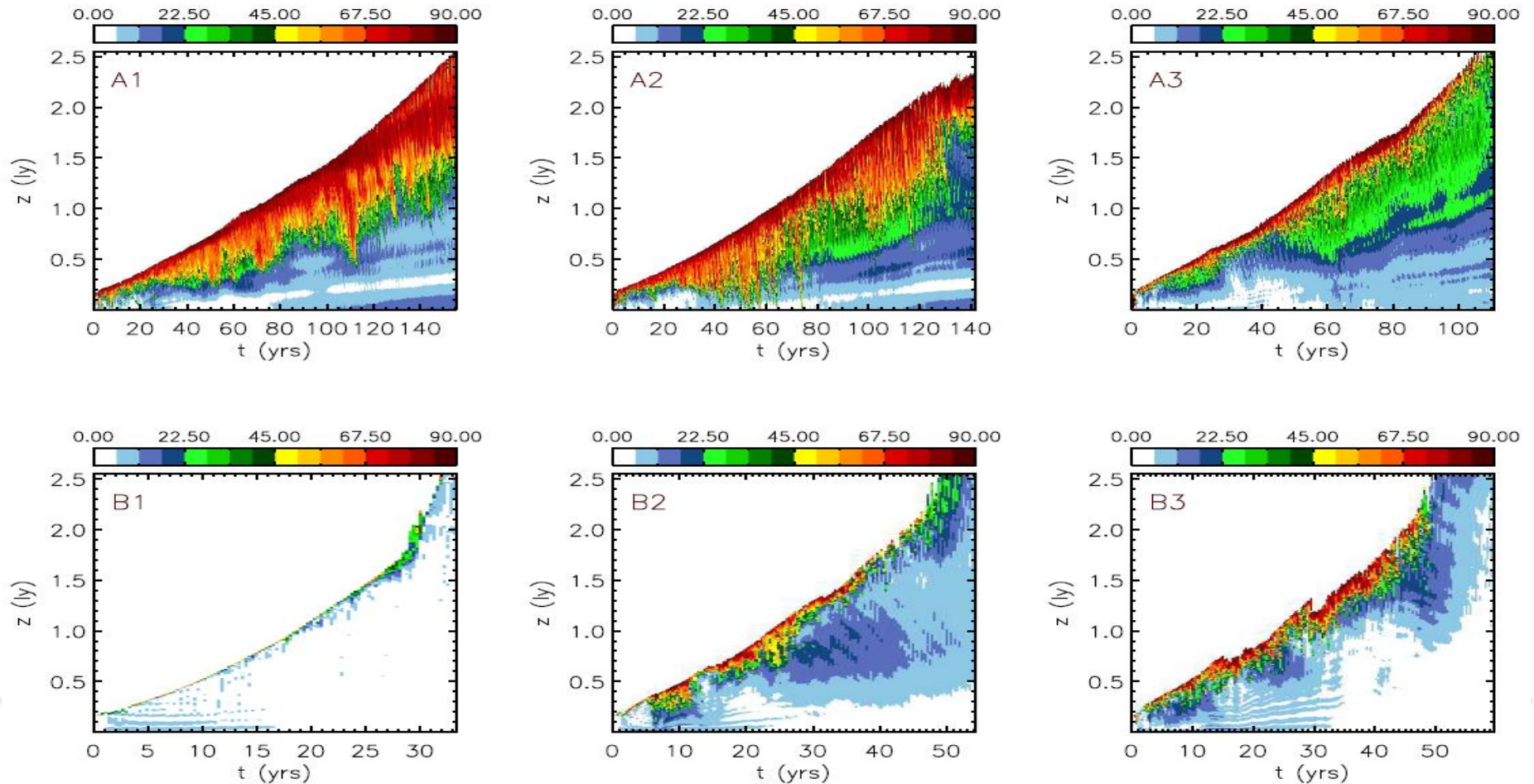


- Case A2 and A3 (low-speed, moderately/highly magnetized) jets show the largest bending (> 20 jet radii);
- Larger Lorentz factors (B2, B3) have a stabilizing effect;
- Weakly magnetized jets (A1, B1) are less affected by the growth of instability;

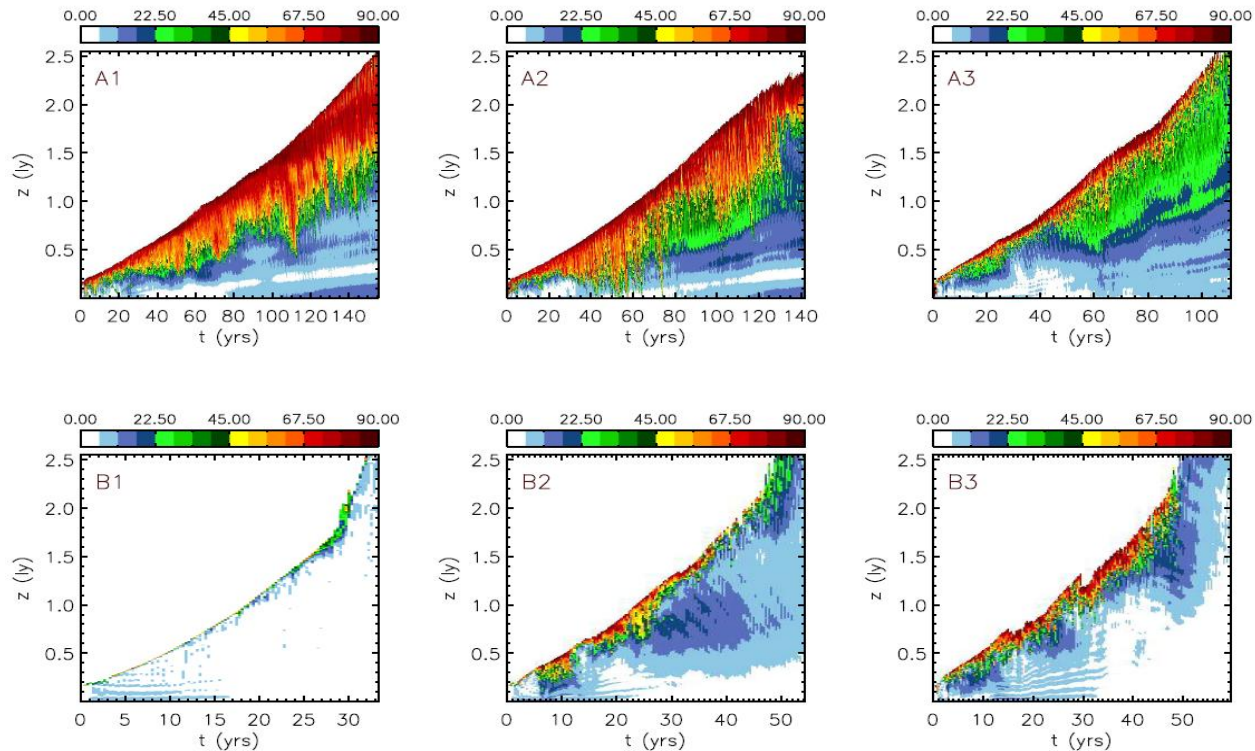
Flow Direction

- Flow direction is measured by computing the average angle of the mass flux vector with vertical direction:

$$\bar{\theta}_{\pm}(z) = \cos^{-1} \left(\frac{\int (v \cdot \hat{z} / |v|) \chi_{\pm} dx dy}{\int \chi_{\pm} dx dy} \right)$$



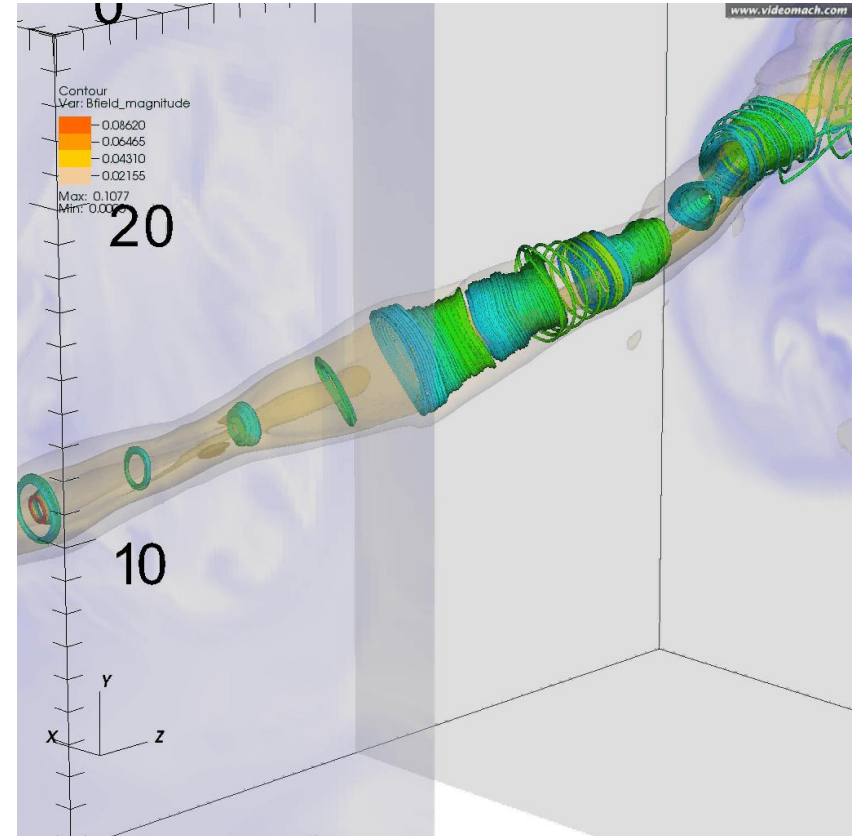
Flow Direction



- Low-speed jets assume a large-scale curved structure;
- High-speed jets more parallel and build kicks in proximity of the jet head;

Magnetic Field

- Magnetic field topology remains mainly toroidal or helical during the propagation;
- Azimuthal field has the effect of “shielding” the core preventing interaction with the surrounding.
- Magnetic field dissipates and becomes turbulent in the cocoon (→ randomization)



Summary

- 3D models of azimuthally confined relativistic jets are very different from 2D axisymmetric models:
 - Kink-unstable non-axisymmetric structures with large time-variability;
 - Large σ ($\gtrsim 1$) leads to considerable jet deflections;
 - Pronounced asymmetric backflows;
 - Jet wiggling progressively more pronounced towards the jet head
 - Multiple strong shocks are formed by change of direction;
 - Low-speed ($\gamma \lesssim 2$), moderately/highly magnetized jets ($\sigma \simeq 1-10$) are promising candidates for explaining the morphology of the Crab jet.
 - Future models will consider the jet-torus connection in 3D
-

Thank you